*Korean J. Chem. Eng.*, 34(9), 2548-2558 (2017)
DOI: 10.1007/s11814-017-0141-y

pISSN: 0256-1115
eISSN: 1975-7220

# Advanced dual fluidized bed steam gasification of wood and lignite with calcite as bed material

**Florian Benedikt†, Josef Fuchs, Johannes Christian Schmid, Stefan Müller, and Hermann Hofbauer**

TU Wien, Institute of Chemical, Environmental and Biological Engineering, Getreidemarkt 9/166, 1060 Vienna, Austria
(*Received 16 February 2017 • accepted 21 May 2017*)

**Abstract**–This paper presents experimental results with a new generation of a 100 $kW_{th}$ dual fluidized bed steam gasification pilot plant with calcite as bed material, converting wood and lignite in separate test runs into product gas. The results are compared to experiments with the same fuels with olivine as bed material and the previous generation of the gasification pilot plant at TU Wien. The highly catalytic active calcium oxide shifted the product gas composition towards higher hydrogen and carbon dioxide and lower carbon monoxide content. The tar amount was decreased and the tar composition changed, resulting in lower tar dew points. The dust content in the product gas was reduced with the advanced pilot plant design with calcite in comparison to the classic design with olivine. Therefore, attrition of bed material was decreased by utilizing the advanced design and calcite with its benefits can be used without profuse continuous replacement of bed material.

Keywords: DFB Steam Gasification, Advanced 100 kW Pilot Plant, Calcite, Wood, Lignite

## INTRODUCTION

Thermo-chemical conversion of biogenic feedstock is a promising option to enable eco-friendly and efficient production of heat and power, secondary energy carriers and valuable products. Dual fluidized bed (DFB) steam gasification has long been subject of investigations at TU Wien. This technology has been demonstrated at industrial scale in (i) Güssing, Austria (8 $MW_{th}$ fuel power) [1], (ii) Oberwart, Austria (8.5 $MW_{th}$) [2], (iii) Senden, Germany (15 $MW_{th}$) [3] and (iv) Gothenburg, Sweden (30 $MW_{th}$) [4]. The aim of the DFB steam gasification is the production of a nitrogen-free medium calorific product gas from biogenic feedstock. The technology also offers a promising possibility for the production of a synthesis gas from fossil fuels like lignite. Fluidized bed systems offer the benefit of a high fuel flexibility compared to, e.g., entrained flow systems with oxygen and steam as gasification medium. Furthermore, the production of pure oxygen for entrained flow systems leads to a high energy demand and, therefore, high costs. Whereas no pure oxygen is necessary for DFB steam gasification, DFB systems use a bed material to ensure uniform conversion of the feedstock on the one hand, and to act as a transport medium for char and heat on the other hand. The mentioned industrial plants use olivine as bed material, which is an iron-magnesium-silicate-based mineral in the earth's subsurface. Olivine offers several advantages (including high attrition resistance, moderate catalytic activity regarding tar reforming and a high heat capacity) for usage in fluidized bed steam gasification, but is comparably expensive and not available all over the world. Therefore, the investigation of cheap alternative bed materials (like calcite) is a subject of research at TU Wien. Calcite is a well-known material which offers several advantages like high catalytic activity, low material costs and worldwide abundancy. Nevertheless, it brings along one major disadvantage for usage in fluidized beds: The low attrition resistance leads to problems with classic dual fluidized bed plants. Thus, an advanced concept for the DFB gasification has been proposed by TU Wien, and furthermore an experimental 100 $kW_{th}$ pilot plant was built. The design facilitates the use of calcite as bed material by the application of gentle separation units and further enhances the gas-solid contact and residence time of the product gas through geometrical modifications of the gasification reactor. The effect of using calcite as bed material combined with the advanced design compared to the classic design and olivine as bed material will be discussed within this paper. Therefore, product gas composition, tar contents and performance indicating key figures were investigated.

## MATERIAL AND METHODS

### 1. Classic and Advanced DFB Steam Gasification

The principle of the DFB steam gasification is shown in Fig. 1.

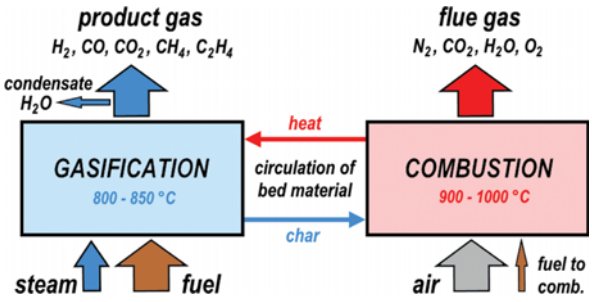


**Fig. 1. Basic principle of the DFB steam gasification.**

†To whom correspondence should be addressed.
E-mail: florian.benedikt@tuwien.ac.at
‡5th International Conference on Gasification and Its Application.
Copyright by The Korean Institute of Chemical Engineers.

Solid fuels are converted into a nitrogen-free product gas, which mainly consists of hydrogen ($H_2$), carbon monoxide (CO), carbon dioxide ($CO_2$), and methane ($CH_4$). The process is based on two interconnected reactors, the gasification reactor (GR) and the combustion reactor (CR). These two reactors are thermodynamically connected via a circulating bed material, which works as heat carrier and supplies the overall endothermic gasification with the necessary heat from the combustion reactor. The main fuel for the combustion reactor itself is provided by the residuals of the gasification, so-called char. With the circulating bed material, this char is transported to the combustion reactor, where it is burned with air. Additional fuel can be introduced into the combustion reactor to control the gasification temperature and to compensate the relatively high specific heat losses of the experimental pilot plant. It is obvious that within this process the flue gas stream is separated from the product gas stream. This leads to a high calorific nitrogen-free product gas.

Based on this principle, several industrial-sized plants have been built and operated with olivine as circulating bed material. Olivine is a common silicate-based mineral in the earth's subsurface, and after several days of operation in a DFB gasification plant, it forms calcium-rich layers on its surface caused by interaction with biomass ash. These calcium-rich layers lead to an increased catalytic activity with respect to tar reduction [5,6]. Thus, many experimental test runs with the classic design of the DFB technology and olivine as bed material have been carried out at TU Wien. Fig. 2 shows the classic design that is typically used at the existing industrial sized plants, which consists of a bubbling fluidized bed as gasification reactor and a fast fluidized bed as combustion reactor. In the following, the classic reactor design is referred to with the abbreviation "a". The reactors are connected via a loop seal or a chute in the lower part of the reactors and a loop seal in the upper part. The bed material, which leaves the combustion reactor, is separated from the flue gas via a cyclone and then introduced into the gasification reactor again. Further information regarding the classic design of the 100 $kW_{th}$ pilot plant at TU Wien can be found in [7].

To improve gas-solid contact within the gasification reactor, an advanced design of the DFB steam gasification process has been developed at TU Wien [8,9] (see Fig. 3). In the following, the advanced reactor design is referred to with the abbreviation "b". The advanced design facilitates the use of pure calcite ($CaCO_3$) as bed material, which is clearly superior regarding tar reduction in comparison to olivine, but compared to commercially applied bed materials for fluidized bed applications, e.g., olivine or silica sand, calcite shows relatively low abrasion resistance. Therefore, the advanced design is equipped with two gravity separators on top of the reactors. Compared to the use of cyclones, the gas and particle velocities are lower, which leads to smooth separation of the calcite from the gas streams. Therefore, also calcite can be used without profuse continuous replacement of the bed material. Cyclones are installed

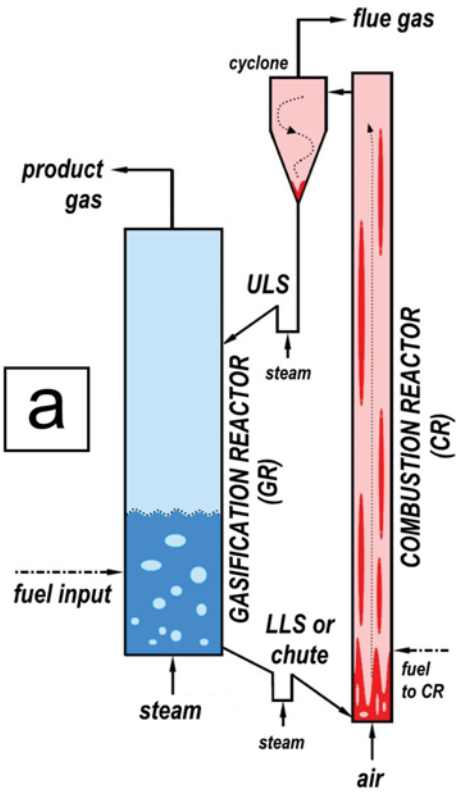


Fig. 2. The classic design of the DFB 100 $kW_{th}$ pilot plant at TU Wien.

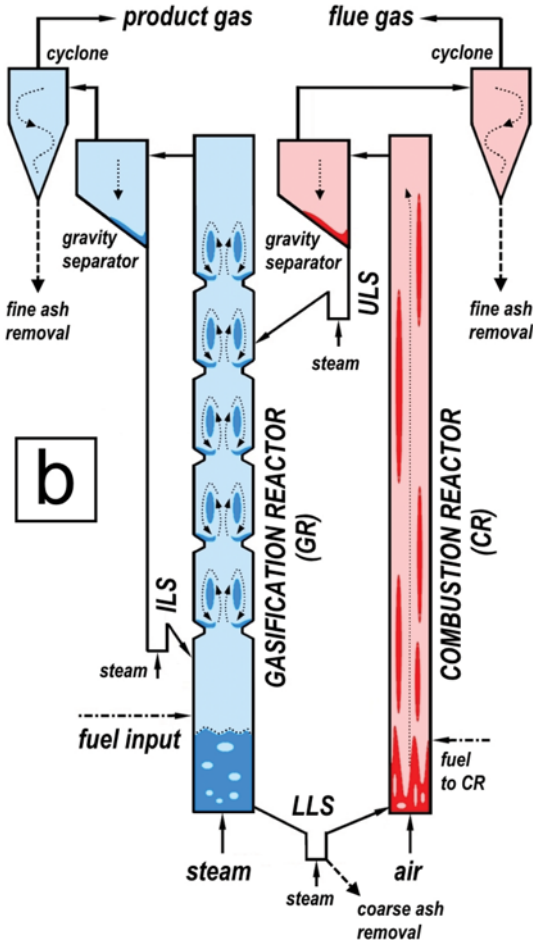


Fig. 3. The advanced design of the DFB 100 $kW_{th}$ pilot plant at TU Wien.

to remove fines after the gravity separators. Besides these developments regarding separators, the key innovation concerns the design of the gasification reactor. The gasification reactor consists of two main parts. The lower part with the fuel input is operated as bubbling fluidized bed. The upper part is designed as a countercurrent column with turbulent fluidized bed zones. The countercurrent column results from the hot bed material, which is separated from the flue gas stream and is introduced into this column. Further, the column is equipped with constrictions, which leads to an increased bed material hold-up over the height of the column. As a result, the interaction of bed material and the product gas in the upper part of the gasification reactor is increased significantly.

## 2. Advanced 100 $kW_{th}$ Pilot Plant at TU Wien

For experimental investigations, an advanced 100 $kW_{th}$ fuel power gasification pilot plant based on the advanced design was built. The plant went into operation in 2014 with several test runs having been conducted so far [10-13]. A basic flow sheet of the pilot facility can be found in Fig. 4. The arrows inside the scheme show flow paths of the solid streams and gas/fluid flows. Important plant parts of the main units are visible and a division into three main cate-

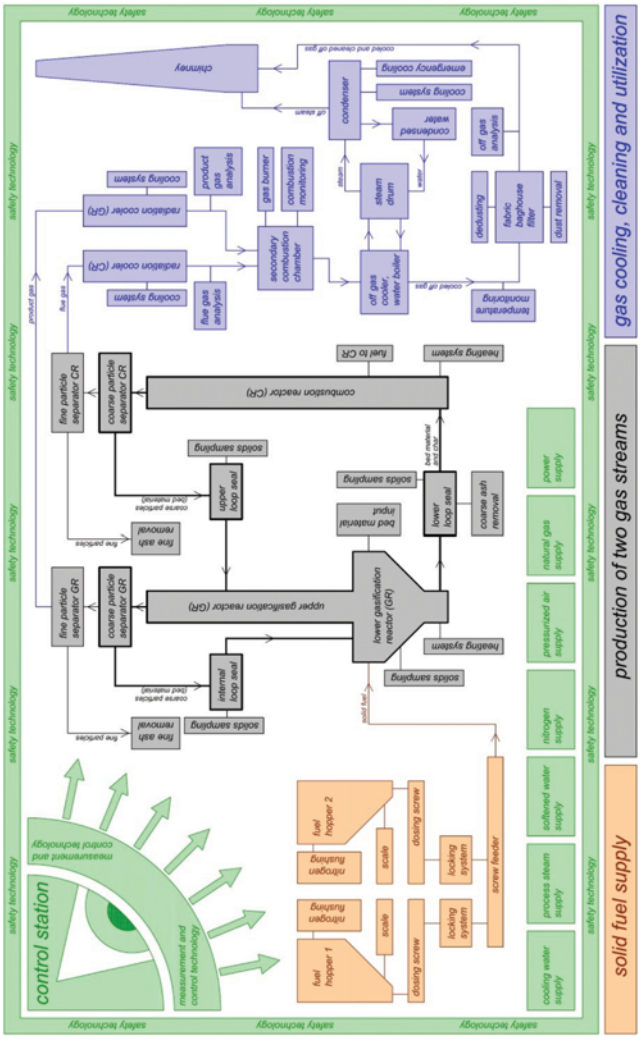


**Fig. 4. Basic flow sheet of the advanced pilot facility at TU Wien.**

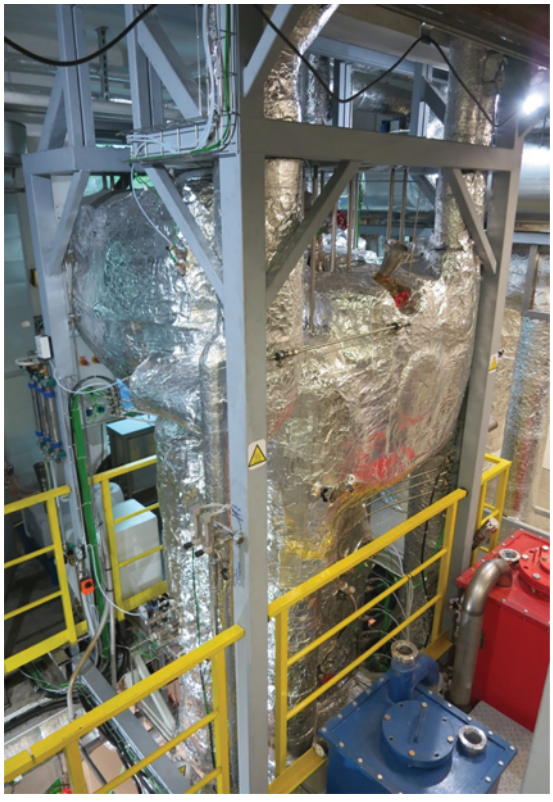

**Fig. 5. Photograph of the upper part of the advanced pilot facility at TU Wien.**

**Fig. 6. Photograph of the lower part of the advanced pilot facility at TU Wien.**

gories is given: solid fuel supply, production of two gas streams, and gas cooling, cleaning and utilization. Additionally, process media supply systems, measurement and control technology, the control station, and an encompassing safety technology, are displayed. Pictures of the pilot facility are shown in Fig. 5 and 6. The height of the combustion reactor is 4.7 m with a diameter of 125 mm, the height of the total gasification reactor exceeds 4.3 m. The overall construction of the reactor system has a height of about 7 m. A control room enables the operator to control all important input streams and parameters.

For safety reasons and to control the operation, the plant is equipped with a programmable logic controller (PLC). The PLC gathers and records all measured data (e.g., temperatures, pressures, gas compositions). To guarantee effective process control and a detailed insight into the gasification process, more than 100 temperature and 70 pressure sensors were installed. Within each main part of the new pilot plant, technical improvements were implemented. To ensure smooth operation of the fluidized bed, the hopper and fuel feeding system is an important part. Special arrangements of screws, cooling jackets and two hoppers to mix different fuels were constructed. Three staged air nozzles are used for the combustion reactor and allow an adjustment of the air-to-fuel ratio independently from the overall bed material circulation rate. For the gasification of difficult fuel types with increased efficiency, the gas/particle interaction is significantly enhanced due to the upper gasification reactor and its geometrical modifications. It is possible to change the geometry of the constrictions inside the upper gasification reactor. So it is possible to guarantee an optimization of the fluid dynamics without influencing the desired constant production of the product gas volume flow. The two reactors are connected via the lower loop seal (LLS) and the upper loop seal (ULS) and therefore prevent gas leakages between the two reactors. Further, multistage solid separation equipment (coarse particle separator and fine particle separator) ensures low fine content on each gas flow path. In contrast to cyclones, the constructed coarse particle separator is carried out as a gravity separator, which exerts low attrition and abrasion effects to the bed material. Bed material from the gravity separator of the gasification is returned via the internal loop seal (ILS). Special equipment enables bed material samples from different locations. Coarse and fine ash removal systems via screws and closed ash hoppers are implemented as well. During the test runs, main product gas components like hydrogen, carbon monoxide, carbon dioxide and methane are analyzed online by a Rosemount NGA2000 gas analyzer. Further product gas components like ethene are measured by a gas chromatograph (Perkin Elmer ARNEL - Clarus 500) every 15 min. To avoid any damage of the measurement equipment, the product gas has to be filtered and washed with rapeseed methyl ester (RME) to remove condensable components like water and tars. The online gas measurement equipment is displayed in Fig. 7.

The determination of solid particles and higher hydrocarbons (tar) in product gas takes place discontinuously. Solid particles (dust and char) are sampled with a small cyclone and a quartz wool stuffed filter cartridge. Tar is sampled isokinetically with impinger bottles, and afterwards gravimetric as well as tars detected by gas chromatography mass spectrometry (GCMS) are determined. The

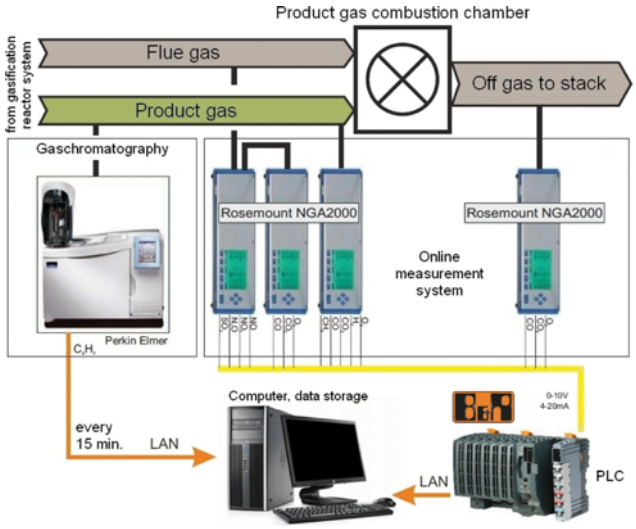


**Fig. 7. Online gas measurement equipment, modified from Schmalzl [14].**

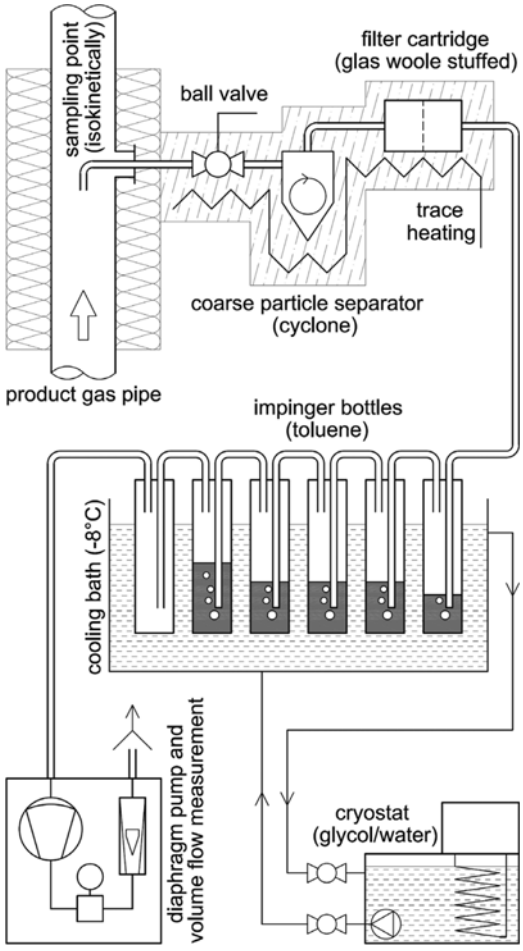


**Fig. 8. Tar, dust, char, and water sampling scheme for the advanced pilot plant.**

measurement method is based on [15], which aims at the determination of tars originating from biomass gasification. Typically, iso-

propanol is used as solvent, but for measurements at the advanced pilot plant, toluene is used, because the solubility for tar in toluene is generally higher and the water content in the product gas can be measured simultaneously. With this setup, the detection of toluene is impossible and the detection of benzene and xylene is not easy. Therefore, all GCMS tar values in this paper are presented without benzene, toluene and xylene (BTX). The sampling scheme for tar, dust, char and water is shown in Fig. 8.

**3. Investigated Bed Materials**

The presented experiments of the advanced 100 $kW_{th}$ pilot plant in this paper were conducted with pure calcite ($CaCO_3$) as bed material. The experimental results were compared to results with the classic pilot plant with olivine as bed material. The main components of the used bed materials are given in Table 1. Regarding Mohs scale for mineral hardness, olivine has a value of 6-7 and calcite around 3. Due to the high temperature in the gasification system, the bed material was calcined. The initial bed material inventory calcite was calcined in the reactor system due to adjusted operating conditions at high temperatures. Through a release of $CO_2$, a change of bed material density occurred. Thus, the practically active bed material mainly consists of calcium oxide (CaO) and some minor impurities like MgO.

**4. Feedstock for Experimental Test Runs**

Two separate test runs with wood pellets and lignite were conducted with the advanced 100 $kW_{th}$ pilot plant. The proximate and ultimate analysis of both fuel types are given in Table 2. Wood pellets according to the Austrian standard ÖNORM M 7135 and lignite of the same batch used in previous investigations presented in [16] were used for gasification test runs. Due to the longer storage time, the water content of lignite decreased from 18.6 mass-% [16] to 13.0 mass-%.

**Table 1. Main components of the used bed materials for DFB steam gasification**

| Name/parameter | Unit | Olivine | Calcite |
|---|---|---|---|
| $CaCO_3$ | $wt\%_{db}$ | - | 95-97 |
| CaO | $wt\%_{db}$ | <0.4 | - |
| $MgCO_3$ | $wt\%_{db}$ | - | 1.5-4.0 |
| MgO | $wt\%_{db}$ | 48-50 | - |
| $SiO_2$ | $wt\%_{db}$ | 39-42 | 0.4-0.6 |
| $Al_2O_3$ | $wt\%_{db}$ | - | 0.2-0.4 |
| $Fe_2O_3$ | $wt\%_{db}$ | 8-11 | 0.1-0.3 |

**Table 2. Proximate and ultimate analysis of feedstock for experiments with the advanced 100 $kW_{th}$ pilot plant**

| Name/parameter | Unit | Wood | Lignite |
|---|---|---|---|
| Water content | mass-% | 7.2 | 13.0 |
| Ash content | $mass\text{-}\%_{db}$ | 0.2 | 4.23 |
| Carbon (C) | $mass\text{-}\%_{db}$ | 50.7 | 65.53 |
| Hydrogen (H) | $mass\text{-}\%_{db}$ | 5.9 | 3.75 |
| Nitrogen (N) | $mass\text{-}\%_{db}$ | 0.2 | 0.84 |
| Oxygen (O) | $mass\text{-}\%_{db}$ | 43.0 | 25.22 |
| Sulphur (S) | $mass\text{-}\%_{db}$ | 0.005 | 0.38 |
| Chlorine (Cl) | $mass\text{-}\%_{db}$ | 0.005 | 0.05 |
| Volatile matter | $mass\text{-}\%_{db}$ | 85.5 | 51.8 |
| Fixed carbon | $mass\text{-}\%_{db}$ | 14.5 | 48.2 |
| Lower heating value (LHV) | MJ/kg | 17.4 | 20.8 |

**5. Mass and Energy Balance with IPSEpro**

For evaluation and validation of the process data, which was gathered during the experiments, the software package IPSEpro was used. IPSEpro is a software package originating from the power plant sector, which offers stationary process simulation based on flow sheet modelling. A comprehensive model library for biomass gasification was developed by Pröll and Hofbauer [17]. It enables the user to calculate data, which cannot be measured directly, via mass and energy balances. Furthermore, calculations allow the validation of the measured data and therefore all presented results are highly valuable and representative.

**6. Performance Indicating Key Parameters**

The process performance was evaluated according to the presented key parameters in this subsection. The steam to fuel ratio $\varphi_{SF}$ (Eq. (1)) expresses the sum of fluidization steam and fuel water in relation to the total mass of dry and ash-free fuel introduced into the GR. As, initially, the steam is used for the gasification of carbon and to enable comparison between gasification of fuels with different fuel composition, the steam to carbon ratio $\varphi_{SC}$ (Eq. (2)) is commonly used. The fuel-related water conversion $X_{H_2O,fuel}$ (Eq. (3)) gives the amount of water consumed per mass unit of converted fuel during gasification, whereas the steam-related water conversion $X_{H_2O}$ (Eq. (4)) gives the relation of water consumed and water introduced into the GR. The carbon conversion in the GR $X_C$ (Eq. (5)) is the ratio of the amount of carbon leaving the GR via the product gas to the amount of carbon introduced into it with the fuel. The cold gas efficiency $\eta_{CG}$ (Eq. (6)) gives the amount of chemical energy in the product gas related to the chemical energy in the fuel, which is introduced into the GR based on the LHV.

$$\varphi_{SF}=\frac{\dot{m}_{steam}+x_{H_2O,fuel}\cdot\dot{m}_{fuel}}{(1-x_{H_2O,fuel}-x_{ash,fuel})\cdot\dot{m}_{fuel}} \quad \text{steam to fuel ratio} \quad (1)$$

$$\varphi_{SC}=\frac{\dot{m}_{steam}+x_{H_2O,fuel}\cdot\dot{m}_{fuel}}{x_{C,fuel}\cdot\dot{m}_{fuel}} \quad \text{steam to carbon ratio} \quad (2)$$

$$x_{H_2O,fuel}=\frac{\dot{m}_{steam}+x_{H_2O,fuel}\cdot\dot{m}_{fuel}-x_{H_2O,PG}\cdot\dot{m}_{PG}}{(1-x_{H_2O,fuel}-x_{ash,fuel})\cdot\dot{m}_{fuel}} \quad (3)$$

fuel-related water conversion

$$x_{H_2O}=\frac{\dot{m}_{steam}+x_{H_2O,fuel}\cdot\dot{m}_{fuel}-x_{H_2O,PG}\cdot\dot{m}_{PG}}{\dot{m}_{steam}+x_{H_2O,fuel}\cdot\dot{m}_{fuel}} \quad (4)$$

steam-related water conversion

$$x_C=\frac{x_{C,PG}}{x_{C,fuel}\cdot\dot{m}_{fuel}} \quad \text{carbon conversion in the GR} \quad (5)$$

$$\eta_{CG}=\frac{\dot{V}_{PG}\cdot LHV_{PG}}{\dot{m}_{fuel}\cdot LHV_{fuel}}\cdot 100 \quad \text{cold gas efficiency} \quad (6)$$

Regarding the composition of the product gas, the water gas shift reaction (Eq. (7)) is the most important heterogeneous catalyzed gas-gas reaction occurring in the product gas. Steam reforming of hydrocarbons (Eq. (8)) is introduced to discuss tar reduction.

$$CO+H_2O \rightleftharpoons CO_2+H_2 \quad \text{water gas shift reaction} \quad (7)$$

**Table 3. Classification of tar by physical properties and list of considered compounds within this study**

| Tar class | Class name | Property | Compounds considered in this study |
|---|---|---|---|
| 1 | GC-undetectable | Very heavy tars, cannot be detected by GC | None |
| 2 | Heterocyclic | Tars containing heteroatoms; highly water soluble | Benzofurane, 2-methylbenzofurane, dibenzofurane, chinoline, isochinoline, indole, carbazole, methylpyiridine, 1-benzothiophene, dibenzothiophene, phenol, methylphenole, dimethylphenole, eugenole, isoeugenole |
| 3 | Light aromatic | Light hydrocarbons with single ring; not problematic in terms of condensation and water solubility | Phenylacetylene, styrene, mesitylene, ethylbenzene, xylene |
| 4 | Light polyaromatic | 2- and 3-ring compounds; condense at intermediate temperatures at relatively high temperatures | 1H-indene, 1-indanone, naphthalene, methylnaphthalene, vinylnaphthalene, biphenyle, acenaphthylene, acenaphthene, fluorene, anthracene, phenanthrene, methylphenanthrene, methylanthracene |
| 5 | Heavy polyaromatic | Larger than 3-ring compounds; condense at high temperatures at low concentrations | Fluoranthene, pyrene, benzo[a]anthracene, chrysene, benzo[b]fluoranthene, benzo[k]fluoranthene, benzo[a]pyrene, benzo[e]pyrene, benzo[g,h,i]perylene, dibenz[a,h]anthracene, indeno[1,2,3-cd]pyrene, perylene, coronene |

$$C_aH_b + a\ H_2O \rightleftharpoons a\ CO + \left(a + \frac{b}{2}\right)H_2 \quad (8)$$

steam reforming of hydrocarbons

The catalytic activity of the bed material combined with the innovative gasifier design promotes besides other reactions also the water gas shift reaction. The extent of the promotion can be expressed by the logarithmic deviation from chemical equilibrium $p\delta_{eq,\,WGS}$ (Eq. (9)).

$$p\delta_{eq,\,WGS} = \log_{10}\left[\frac{\Pi_i p_i^{\nu_i}}{K_{p,\,WGS}(T)}\right] \quad (9)$$

logarithmic deviation from water gas shift equilibrium

The equilibrium constant $K_{p,\,WGS}(T)$ was calculated using the commercial software HSC [18]. If $p\delta_{eq,\,WGS}=0$, the water gas shift reaction equilibrium is fulfilled. If $p\delta_{eq,\,WGS}<0$, the actual state is still on the side of the reactants, so further reaction is thermodynamically possible. If $p\delta_{eq,\,WGS}>0$, the actual state is on the side of the products, which can thermodynamically not be reached due to the water gas shift reaction alone, but by, e.g., intermediate products from devolatilization of higher hydrocarbons. Generally, a higher activity in terms of the water gas shift reaction also leads to higher activity regarding reforming of hydrocarbons [19].

**7. Tar Classification and Calculation of the Tar Dew Point**

Tar components can be classified according to many different aspects. One possible way is according to temperature of formation suggested by Milne et al. [20] into primary, secondary and tertiary tar components. Wolfesberger et al. introduced a classification system according to superordinate groups [21]. Table 3 determines the classification of tar by physical properties as suggested by Rabou et al. [22] and lists considered GCMS components within this study.

The tar dew point is an important value for fouling and therefore a major consideration for long-term operation of biomass gasification systems as it facilitates an evaluation of the potential impact on downstream equipment. The tar dew point was calculated via the tar dew point model developed by the Energy Research Centre of the Netherlands (ECN) [23].

## RESULTS AND DISCUSSION

Table 4 lists the main operating parameters of the gasification

**Table 4. Main operating parameters for gasification of wood and lignite**

| Value | Unit | Experiment | | | |
|---|---|---|---|---|---|
| | | 1a [7] | 1b | 2a [16] | 2b |
| DFB plant design | | Classic | Advanced | Classic | Advanced |
| Fuel type to GR | | Wood | Wood | Lignite | Lignite |
| Fuel power to GR | kW | 90 | 101 | 90 | 100 |
| Fuel feeding position GR | | In-bed | On-bed | In-bed | On-bed |
| Initial bed material | | Olivine | Calcite | Olivine | Calcite |
| Gasification temperature | °C | 850 | 797 | 850 | 839 |
| Steam to fuel ratio ($\varphi_{SF}$) | $kg_{H_2O}/kg_{fuel,\,daf}$ | 0.6 | 0.7 | 0.9 | 1.0 |
| Steam to carbon ratio ($\varphi_{SC}$) | $kg_{H_2O}/kg_C$ | 1.3 | 1.4 | 1.3 | 1.5 |

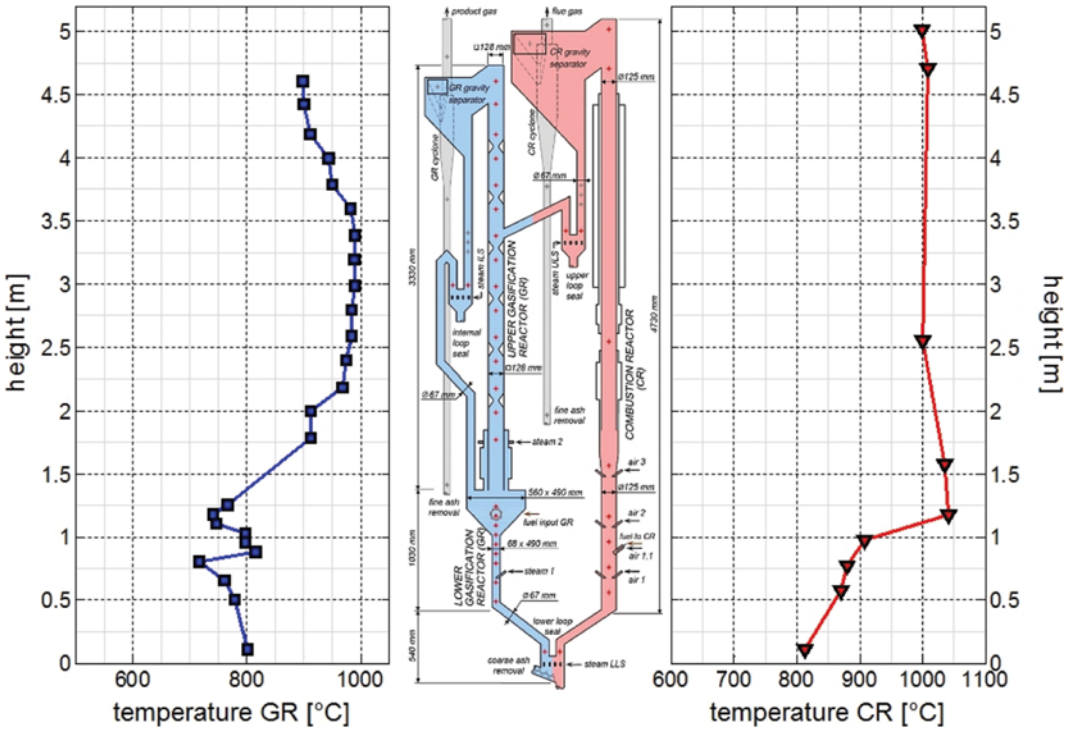


**Fig. 9. Overview on the average temperature profiles for the gasification (left) and combustion (right) reactor for the gasification test run with wood operating the advanced 100 $kW_{th}$ pilot plant with calcite as bed material (experiment 1b).**

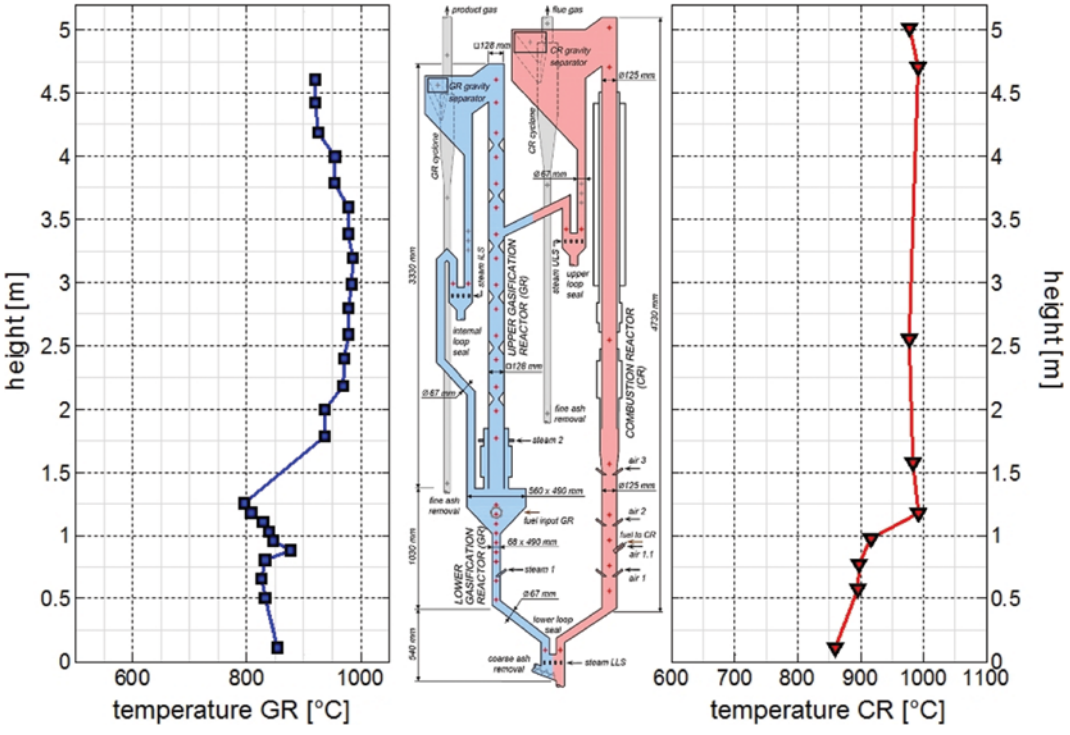


**Fig. 10. Overview on the average temperature profiles for the gasification (left) and combustion (right) reactor for the gasification test run with lignite operating the advanced 100 $kW_{th}$ pilot plant with calcite as bed material (experiment 2b).**

test runs of wood and lignite. Figs. 9 and 10 show an overview on the average temperature profiles over the steady state operation in the combustion and gasification reactor for gasification of wood and lignite, respectively. Due to the different fuel properties, (see Table 2) dissimilar temperature profiles were observed during the test runs with the advanced pilot plant (experiments 1b and 2b).

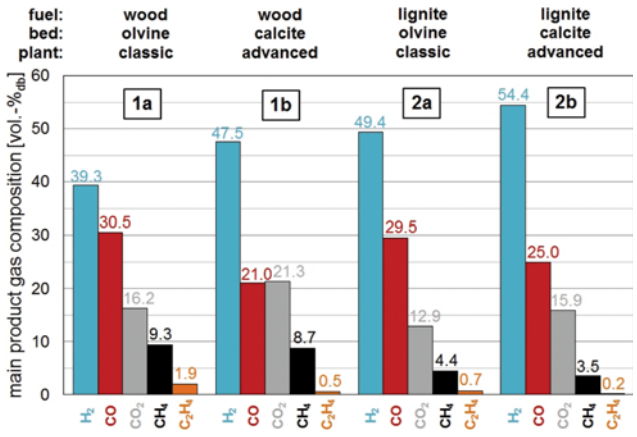


**Fig. 11. Product gas composition for gasification of wood and lignite.**

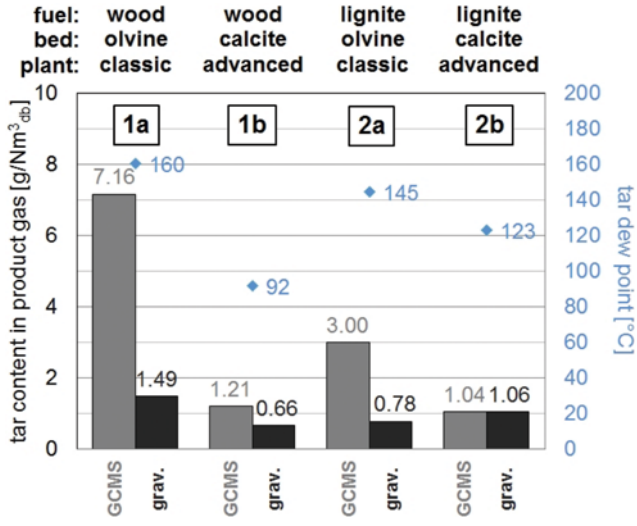


**Fig. 12. Tar content and calculated dew point of the product gas for gasification of wood and lignite.**

The average temperature difference between the gasification and combustion reactor was smaller for the gasification test run with lignite, because of its high share of fixed carbon. The high amount of fixed carbon was not as easily devolatilized and gasified in the

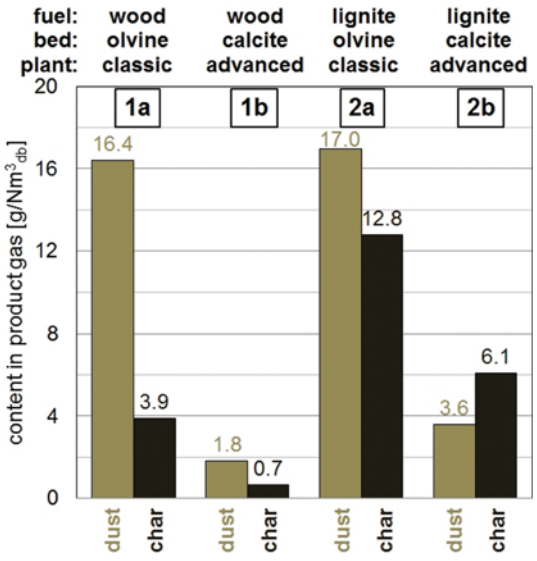


**Fig. 13. Dust and char content of the product gas for gasification of wood and lignite.**

gasification reactor and, therefore, more char was transported to the combustion reactor. This allowed a low input of additional fuel into the combustion reactor. Thus, the char enabled a smooth combustion in the combustion reactor, which can be seen through a narrow temperature profile for the gasification of lignite. In addition, the temperature profile in the gasification reactor with lignite as fuel showed a more homogeneous behavior over the height than for wood as fuel. Figs. 11, 12 and 13 show the product gas composition as well as the related tar, dust and char content for gasification of wood and lignite with olivine and calcite as bed material (experiments 1a, 1b, 2a and 2b). For all shown test runs, the steam to carbon ratio was kept in a comparable range of 1.3-1.5 kg/kg. Table 5 presents the performance indicating key parameters and additional key data for the gasification experiments. The tar components were classified according to Table 3 and their shares are shown in Fig. 14.

**1. Experimental Results for Gasification of Wood**

The gasification test runs with wood and calcite as bed material (advanced plant design: experiment 1b) were compared with test runs carried out with the previous 100 $kW_{th}$ pilot plant using

**Table 5. Key parameters for gasification of wood and lignite**

| Value | Unit | Experiment | | | |
|---|---|---|---|---|---|
| | | 1a [7][a] | 1b | 2a [16][a] | 2b |
| Specific product gas yield | $Nm^3_{db}/kg_{fuel,daf}$ | 1.04 | 1.36 | 1.65 | 1.62 |
| Product gas power | kW | 68.4 | 85 | 66.8 | 70.5 |
| $H_2O$ content in product gas | vol% | 32.6 | 31.6 | 19.1 | 25.1 |
| Fuel-related water conversion $X_{H_2O,fuel}$ | $kg_{H_2O}/kg_{fuel,daf}$ | 0.13 | 0.23 | 0.55 | 0.59 |
| Steam-related water conversion $X_{H_2O}$ | $kg_{H_2O}/kg_{H_2O}$ | 0.22 | 0.31 | 0.61 | 0.58 |
| Carbon conversion in the GR $X_C$ | $kg_{C,PG}/kg_{C,fuel}$ | 0.67 | 0.75 | 0.66 | 0.59 |
| Logarithmic deviation from WGS equilibrium, $p\delta_{eq,WGS}$ | - | −0.34 | −0.03 | −0.01 | 0.02 |
| Cold gas efficiency $\eta_{CG}$ | % | 76 | 84 | 74 | 71 |

[a]Values may vary from the original literature due to different calculation methods. All values within this work are calculated consistently

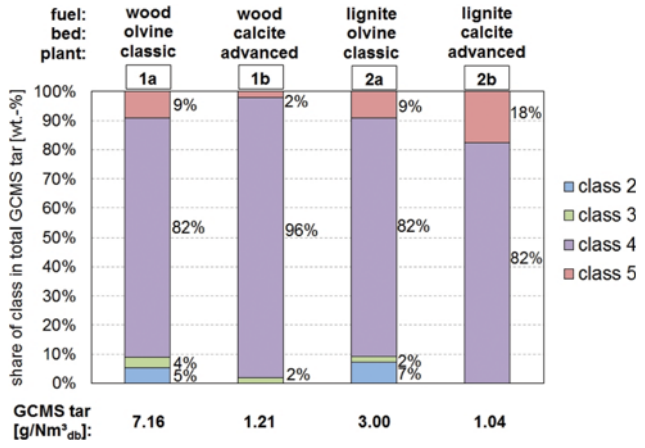


**Fig. 14. Total GCMS tar in g/Nm$^3_{db}$ and shares of tar components according to the classification of Table 3 for gasification of wood and lignite.**

olivine as bed material (classic plant design: experiment 1a) [7]. In spite of lower gasification temperatures, the product gas composition was strongly shifted towards a higher $H_2$ (+8.2 vol%$_{db}$) and $CO_2$ (+5.1 vol%$_{db}$) and a lower CO (−9.5 vol%$_{db}$) content with calcite as bed material. Generally, at lower gasification temperatures, a contrary effect on the gas composition is expected. The change in the product gas composition can be explained by the strong influence of calcium oxide on the heterogeneous catalyzed water gas shift reaction (Eq. (7)). Additionally, gravimetric and GCMS tar contents were remarkably lowered in case of the advanced plant design. There was also a reasonable impact on the $C_2H_4$ content (−1.4 vol%$_{db}$), which seems to be a good indicator of the GCMS tar content in the product gas [24,25]. The decomposition of hydrocarbons probably took place by a coupling of two effects: (i) The more active bed material calcium oxide to enhance steam reforming reactions (Eq. (8)), and (ii) higher temperatures in the countercurrent column for cracking reactions. There were no heterocyclic tar components detected in experiments with calcite as bed material. Both total GCMS tar and the percentage of class 5 tar were significantly lower for experiments at the advanced pilot plant resulting in a very low tar dew point of 92 °C instead of 160 °C (Fig. 12). The logarithmic deviation from chemical equilibrium was significantly lower for experiment 2b and, thereby, equilibrium was nearly fulfilled with calcium oxide as active bed material (Table 5).

The specific product gas yield was noticeably increased (+0.32 Nm$^3_{db}$/kg$_{fuel,daf}$), which could be explained by longer residence times of char particles due to the advanced pilot plant design and calcium oxide as bed material to enhance the water gas shift reaction. Within this reaction, the dry gas volume was increased by the conversion of water. The longer residence time of product gas with bed material and char led to a higher carbon conversion (+8.4%). The increased water conversion can be explained by the stronger catalytic activity of calcium oxide over olivine and longer residence times for particles and, therefore, longer contact times between the product gas and particles in the advanced pilot plant. This resulted in consumption of water by (i) steam reforming and (ii) enhanced water gas shift reaction. and can be noticed in reduced tar amounts and the shifted product gas composition. In addition, when considering the cold gas efficiency (+8%), the advanced pilot plant provided superior results.

The attrition behavior of the bed material is discussed via the dust content in the product gas. As the dust content in the product gas was considerably decreased from 16.4 to 1.8 g/Nm$^3_{db}$ (Fig. 13), there is no concern for major bed material attrition with $CaCO_3$/CaO as bed material when utilizing the advanced design. Note that fine ash and fly char are separated from the product gas with a gravity separator and a cyclone in the advanced pilot plant (see Fig. 3), and there was no separation system installed in the classic design (see Fig. 2). The fine ash removal of the advanced pilot plant was not considered within this paper, as it should be led back to the reactor system in an industrial application.

**2. Experimental Results for Gasification of Lignite**

The results for gasification test runs with lignite and calcite as bed material (advanced plant design: experiment 2b) were compared to test runs carried out with the previous 100 kW$_{th}$ pilot plant using olivine as bed material (classic plant design: experiment 2a) [16]. The product gas composition was strongly shifted towards higher $H_2$ (+5.0 vol%$_{db}$) and $CO_2$ (+3.0 vol%$_{db}$) and lower CO (−4.5 vol%$_{db}$) content with calcite as bed material (Fig. 11). GCMS tar values were comparatively lower for the advanced pilot plant, but the gravimetric tar was in the same range (Fig. 12). Again, a direct correlation between $C_2H_4$ content and GCMS tar was observed. There were no heterocyclic and light aromatic (class 2 and 3) tar components detected in experiment 2b (Fig. 14), and the tar dew point was lowered from 145 to 123 °C. For both experiments with lignite, the product gas composition was very close to water gas shift equilibrium. For experiment 2b, the logarithmic deviation was even positive. When comparing the performance indicating key parameters, the differences between experiment 2a and 2b were minimal for product gas yield, water and carbon conversion and cold gas efficiency (Table 5). The reason could be that lignite possesses very good fuel properties for the DFB steam gasification process: the low content of volatile matter in the fuel composition of lignite resulted even with the catalytically weaker (but still active) olivine in high water and carbon conversions. Thus, the advanced design with more intense contact and longer residence time of catalytic active bed material with the product gas did not have a strong impact on its performance. The $H_2O$ content in the product gas was slightly higher for experiment 2b due to the higher steam to carbon ratio, but the water conversions attained similar values for both experiments. The dust content was lowered from 17.0 to 3.6 g/Nm$^3_{db}$ (Fig. 13) with the advanced design, which again supports the idea of the smooth separation of the soft bed material with the advanced design works.

## CONCLUSION

Investigations on steam gasification of wood and lignite with calcite as bed material and an advanced 100 kW$_{th}$ pilot plant were carried out and compared to existing results with the same fuels, but with olivine as bed material and the classic design of the pilot plant. Results achieved are summarized as follows:

(i) The product gas for both fuels was shifted to higher $H_2$ and

$CO_2$ contents as well as lower CO and $C_2H_4$ contents due to the highly catalytic active calcium oxide forcing the water gas shift and steam reforming reactions.

(ii) Tar amounts in the product gas were significantly decreased and the tar dew points calculated from GCMS tar content were remarkably improved, which seems to be a result of stronger steam reforming and cracking of the tar.

(iii) For experiments with wood, the key parameters regarding gasification were considerably improved with $CaCO_3$/CaO as bed material instead of olivine. However, the same key parameters were not notably changed for the comparable test runs with lignite.

(iv) Furthermore, the attrition behavior of the bed materials olivine and $CaCO_3$/CaO was compared via the dust content in the product gas. According to that parameter, the new separator system reduced attrition and dust content in the product gas using the soft calcite/calcium oxide. The advanced pilot plant design enabled calcite around four- to seven-times higher attrition resistance due to the smooth separation equipment installed in the advanced pilot plant.

The experimental test runs presented in this paper aim to introduce a new bed material for gasification in DFB plants. Calcite as bed material, combined with the advanced DFB reactor design, enhanced catalytic activity in terms of product gas composition, tar reduction and partial improvement for gasification-related key parameters. Calcite is a cheap and easily available bed material and, therefore, a promising alternative to commercially applied bed materials like olivine or silica sand. Calcite as bed material and the advanced DFB gasification system offer the possibility to gasify a broad range of alternative fuels for various applications of the product gas.

## ACKNOWLEDGEMENTS

This research did not receive any specific grant from funding agencies in the public, commercial, or not-for-profit sectors.

## ABBREVIATIONS

a : classic reactor design
b : advanced reactor design
BTX : benzene, toluene, xylene
CR : combustion reactor
DFB : dual fluidized bed
ECN : energy research centre of the Netherlands
GC : gas chromatography
GCMS : gas chromatography mass spectrometry
GR : gasification reactor
N : at standard conditions (0 °C and 101.325 kPa)
PLC : programmable logic controller

### Subscripts

ash : ash
C : carbon
db : dry basis
daf : dry and ash-free
fuel : fuel to gasification reactor
$H_2O$ : water
PG : product gas
steam : steam
th : thermal

### Symbols

a, b : stoichiometric factors [-]
$K_{p,\,WGS}$ : equilibrium constant of the water gas shift reaction [-]
LHV : lower heating value [kJ/kg or kJ/m$^3$]
$\dot{m}$ : mass flow [kg/s]
$p_i$ : partial pressure of component i [Pa]
$p\delta_{eq,\,WGS}$ : logarithmic deviation from the water gas shift equilibrium [-]
$\dot{V}$ : volumetric flow [m$^3$/s]
x : mass fraction
$X_C$ : carbon conversion in the gasification reactor [$kg_C/kg_{C,\,fuel}$]
$X_{H_2O}$ : steam-related water conversion [$kg_{H_2O}/kg_{H_2O}$]
$X_{H_2O,\,fuel}$ : fuel-related water conversion [$kg_{H_2O}/kg_{fuel,\,daf}$]
$\eta_{CG}$ : cold gas efficiency [%]
$\nu_i$ : stoichiometric coefficient of component i [-]
$\varphi_{SC}$ : steam to carbon ratio [$kg_{H_2O}/kg_C$]
$\varphi_{SF}$ : steam to fuel ratio [$kg_{H_2O}/kg_{fuel,\,daf}$]

## REFERENCES

1. H. Hofbauer, R. Rauch, K. Bosch, R. Koch and C. Aichernig, Biomass CHP plant Guessing-A success story, in *Pyrolysis and Gasification of Biomass and Waste*, A. V. Bridgewater, CPL Press, Newbury, Berks., UK (2003).
2. V. Wilk and H. Hofbauer, *Fuel Processing Technol.*, **141**, 138 (2016).
3. F. Kirnbauer, F. Maierhans, M. Kuba and H. Hofbauer, State of the art biomass gasification for CHP production - the Ulm plant, in Proceedings of the 2nd Conference on Renewable Energy Gas Technology, Barcelona, Spain (2015).
4. I. Gunnarsson. The GoBiGas project - efficient transfer of biomass to biofuels, in *Proceedings of the International Seminar on Gasification*, Gothenburg, Sweden (2010).
5. F. Kirnbauer, V. Wilk, H. Kitzler, S. Kern and H. Hofbauer, *Fuel*, **95**, 553 (2012).
6. M. Kuba, F. Havlik, F. Kirnbauer and H. Hofbauer, *Biomass Bioenergy*, **89**, 40 (2016).
7. S. Kern, C. Pfeifer and H. Hofbauer, *Chem. Eng. Sci.*, **90**, 284 (2013).
8. J. C. Schmid, T. Pröll, C. Pfeifer and H. Hofbauer, Improvement of gas-solid interaction in dual circulating fluidized bed systems in *Proc. 9th Eur. Conf. Ind. Furn. Boil.*, Estoril, Portugal (2011).
9. J. C. Schmid, C. Pfeifer, H. Kitzler, T. Pröll and H. Hofbauer, A new dual fluidized bed gasifier design for improved in situ conversion of hydrocarbons in *Proc. Int. Conf. Polygeneration Strateg.*, Vienna, Austria (2011).
10. H. A. Pasteiner, Cold flow investigations on a novel dual fluidised bed steam gasification test plant, master thesis, Institute of Chemical, Biological and Environmental Engineering, TU Wien (2015).
11. M. Kolbitsch, *First fuel tests at a novel 100 kWth dual fluidized bed steam gasification pilot plant*, Ph.D. Thesis, Institute of Chemical, Biological and Environmental Engineering, TU Wien (2016).
12. J. C. Schmid, S. Müller and H. Hofbauer, First scientific results with

the novel dual fluidized bed gasification test facility at TU Wien, in *Proceedings of the 24th European Biomass Conference and Exhibition*, Amsterdam, The Netherlands (2016).
13. S. Müller, J. C. Schmid and H. Hofbauer, First results with an innovative biomass gasification test plant, in *Proceedings 3rd International Conference on Renewable Energy Gas Technology (REGATEC)*, Malmö, Schweden (2016).
14. M. Schmalzl, Implementierung der MSR- Technik einer 100 kW DUAL FLUID Versuchsanlage zur Vergasung von Festbrennstoffen, master thesis, Institute of Chemical, Biological and Environmental Engineering, TU Wien (2014).
15. S. V. B. van Paasen, J. H. A. Kiel, J. P. A. Neeft, H. A. M. Knoef, G. J. Buffinga, U. zielke, K. Sjöström, C. Brage, P. Hasler, P. A. Simell, M. Suomalainen, M. A. Dorrington and L. Thomas, *Guideline for sampling and analysis of tar and particles in biomass producer gases*, Report ECN-02-090, ECN (2002).
16. S. Kern, C. Pfeifer and H. Hofbauer, *Fuel Processing Technol.*, **111**, 1 (2013).
17. T. Pröll and H. Hofbauer, *Int. J. Chem. Reactor Eng.*, **6**, A89, available at: http://www.bepress.com/ijcre/vol6/A89 (2008).
18. Outokumpu HSC Chemistry Thermochemical Database, ver 6.1 A Roine - Finland: Outokumpu Research Oy (2002).
19. M. Kuba, F. Kirnbauer and H. Hofbauer, *Biomass Conver. Biorefinery*, **7**, 11 (2016).
20. T. A. Milne, N. Abatzoglou and R. J. Evans, Biomass gasifier "tars": their nature, formation, and conversion, Golden, CO: National Renewable Energy Laboratory (1998).
21. U. Wolfesberger, S. Koppatz, C. Pfeifer and H. Hofbauer, Effect of iron supported olivine on the distribution of tar compounds derived by steam gasification of biomass, in *Proceedings of the International Conference on Polygeneration Strategies* (ICPS11), Vienna, Austria (2011).
22. L. P. L. M. Rabou, R. W. R. Zwart, B. J. Vreugdenhil and L. Bos, Tar in biomass producer gas, the Energy research Centre of the Netherlands (ECN) experience: An enduring challenge (2009).
23. Energy Research Center of the Netherlands (ECN), http://www.thersites.nl/completemodel.aspx (accessed: September 15, 2016).
24. H. Kitzler, *Zweibettwirbelschicht-Dampfvergasung von biogenen, ascheintensiven Brenn- und Reststoffen - Einfluss der Asche auf den Prozess*, Ph.D. thesis, Institute of Chemical, Biological and Environmental Engineering, TU Wien (2013).
25. S. Kern, Gasification and Co-Gasification of Coal, *Biomass and Plastics in a Dual Fluidized Bed System*, Ph.D. Thesis, Institute of Chemical, Biological and Environmental Engineering, TU Wien (2013).